Gamma secretase inhibition promotes hypoxic necrosis in mouse pancreatic ductal adenocarcinoma

Natalie Cook,[1,2] Kristopher K. Frese,[1] Tashinga E. Bapiro,[1,2] Michael A. Jacobetz,[1] Aarthi Gopinathan,[1,2] Jodi L. Miller,[1] Sudhir S. Rao,[3] Tim Demuth,[3] William J. Howat,[1] Duncan I. Jodrell,[1,2] and David A. Tuveson[1,2]

[1]Cancer Research UK Cambridge Research Institute, Robinson Way, Cambridge CB2 0RE, England, UK
[2]Department of Oncology, Cambridge University Hospitals NHS Foundation Trust, Cambridge CB2 0QQ, England, UK
[3]Merck Research Laboratories, Boston, MA 02115

Pancreatic ductal adenocarcinoma (PDA) is a highly lethal disease that is refractory to medical intervention. Notch pathway antagonism has been shown to prevent pancreatic preneoplasia progression in mouse models, but potential benefits in the setting of an established PDA tumor have not been established. We demonstrate that the gamma secretase inhibitor MRK003 effectively inhibits intratumoral Notch signaling in the KPC mouse model of advanced PDA. Although MRK003 monotherapy fails to extend the lifespan of KPC mice, the combination of MRK003 with the chemotherapeutic gemcitabine prolongs survival. Combination treatment kills tumor endothelial cells and synergistically promotes widespread hypoxic necrosis. These results indicate that the paucivascular nature of PDA can be exploited as a therapeutic vulnerability, and the dual targeting of the tumor endothelium and neoplastic cells by gamma secretase inhibition constitutes a rationale for clinical translation.

CORRESPONDENCE
David Tuveson:
david.tuveson@cancer.org.uk

Abbreviations used: GSI, gamma secretase inhibitor; NICD, Notch intracellular domain; PanIN, pancreatic intraepithelial neoplasia; PDA, pancreatic ductal adenocarcinoma.

Pancreatic cancer has a poor prognosis because of late presentation, early metastases, and resistance of tumor cells to conventional treatments such as radiation and chemotherapy. Although surgery can significantly extend survival in the small subset of eligible patients, most patients ultimately relapse and succumb. Indeed, patients with metastatic disease have a median survival of between 2 and 6 mo. Despite extensive investigation, the cytotoxic agent gemcitabine remains the standard of care offering only a modest survival benefit (Burris et al., 1997). In view of these disappointing results, novel therapeutic approaches are desperately needed.

The main subtype of pancreatic cancer is pancreatic ductal adenocarcinoma (PDA; Hezel et al., 2006). Somatic mutations in human PDA involves four canonical genes, including activating mutations in KRAS in >95% of cases (Smit et al., 1988). Additional insights to PDA pathogenesis have come from investigating the dysregulation of pathways operant during pancreatic development. These include the Notch, Wnt, and Hedgehog signaling pathways, which are mutated or up-regulated in most human pancreatic cancers (Jones et al., 2008).

The Notch signaling pathway controls cell fate decisions important for tissue integrity during metazoan development and is aberrantly activated in many carcinomas including pancreatic cancer (Miyamoto et al., 2003). Notch receptors are transmembrane proteins that direct tissue development by influencing cellular differentiation, proliferation, and death. There are four Notch receptors identified in humans and mice, Notch 1–4, and they contain cytoplasmic domains that serve as tethered transcription factors. Notch receptors use a unique signaling mechanism that is initiated by interaction with neighboring cells that bear cell surface ligands such as Delta or Jagged. Once the Notch receptor is engaged, this triggers extracellular proteolysis by TACE and finally culminates in the gamma secretase–dependent intracellular proteolysis and release of the Notch intracellular domain (NICD). NICD translocates to the nucleus where it activates the transcription of Notch target genes.
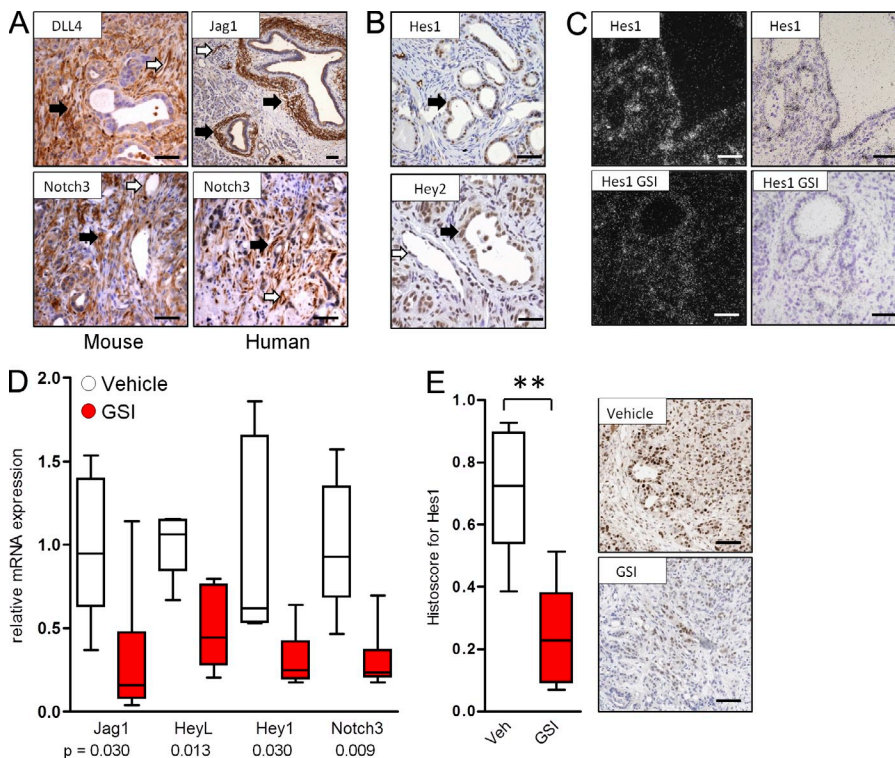
Figure 1. Notch pathway components are expressed in human and mouse PDA and can be decreased by MRK003. (A) Expression of Notch ligands (DLL4 and Jagged1) and receptor (Notch 3) in mouse (left) and human (right) pancreatic cancer specimens ($n = 5$ examined). In addition to the expression in PDA neoplastic cells, note expression in endothelial (white arrows) and stromal cells (black arrows). (B) Expression of Notch target genes Hes1 and Hey2 in mouse PanIN and PDA tissue (neoplastic cells marked by black arrows). Hey2 expression is also noted in intratumoral endothelial cells (white arrow; $n = 5$). (C) In situ hybridization in dark and light fields demonstrating Hes1 expression in pancreatic cancer ductal cells and decreased Hes1 expression upon treatment with MRK003 (GSI; $n = 3$). (D) Quantitative real-time PCR showing relative mRNA expression of Notch pathway components in PDA tissue from mice treated with vehicle ($n = 5$) or MRK003 ($n = 6$) for 10 d. (E) Expression of Hes1 protein in tumors of mice treated with vehicle ($n = 8$) or GSI ($n = 6$; **, $P = 0.003$). Representative images from GSI treated and untreated tumors are shown to the right. Error bars represent SEM. Bars, 100 µm.

In normal adult pancreas, Notch and its ligands are expressed in low or undetectable levels (Miyamoto et al., 2003). In preinvasive pancreatic intraepithelial neoplasia (PanIN) and fully invasive PDA there are prominent elevations in expression of these factors and an associated induction of transcriptional target genes, such as HES-1 (Hairy and Enhancer of Split 1), consistent with activation of this pathway during malignant progression (Miyamoto et al., 2003). Mouse models have implicated Notch activation in pancreatic centroacinar cells, a proposed precursor cell of PDA (Hingorani et al., 2003; Stanger et al., 2005). Additionally, a transgenic mouse model of acinar metaplasia implicated the critical importance of Notch signaling in neoplasia, as the gamma secretase inhibitor (GSI) DAPT reversed the in vitro phenotype of acinar cell trans–differentiation and transformation (Miyamoto et al., 2003). Finally, a recent investigation used the GSI MRK003 to demonstrate selective cytotoxicity against human pancreatic cancer cells in culture and the prevention of pancreatic cancer formation in a mouse model (Plentz et al., 2009).

Given the importance of oncogenic K-ras in pancreatic cancer tumorigenesis and the requirement for Notch signaling in Ras transformation, Notch pathway inhibition is a logical therapeutic target for pancreatic cancer patients (Fitzgerald et al., 2000). As prior studies focused on the prevention of pre-neoplastic progression, we sought to determine the activity of GSI in mice with radiologically evident invasive PDA. Accordingly, we used the KPC mouse model of PDA, a model which recapitulates the cardinal pathophysiological aspects of human PDA and is based upon the pancreatic specific endogenous expression of Kras^{G12D} and Trp53^{R172H} alleles

(Hingorani et al., 2005). The KPC model has previously accurately predicted the failure of gemcitabine (Olive et al., 2009) and the activity of CD40 ligand immunotherapy (Beatty et al., 2011) in patients; therefore, KPC mice with established tumors were used to evaluate the cell–intrinsic and microenvironment effects of GSI treatment. We find that GSI is partially active as a monotherapy in affecting both neoplastic and endothelial cells, but the magnitude of these effects only becomes preclinically evident by the co-administration of gemcitabine. An evaluation of the PDA tissue demonstrates that the sparse intratumoral endothelial cells serve as a major target of GSI and gemcitabine combination treatment, revealing a novel combination to consider for clinical translation.

RESULTS AND DISCUSSION
The Notch pathway is activated in human and mouse PDA and can be inhibited by a GSI

Consistent with prior studies (Hingorani et al., 2003; Miyamoto et al., 2003), we used immunohistochemistry and in situ hybridization to confirm that many components of the Notch pathway were present in neoplastic and microenvironment cells in mouse and human PanIN and PDA specimens (Fig. 1, A–C). Indeed, DLL4 and Jagged1 were detected in both the vasculature and stromal cells surrounding neoplastic cells (Fig. 1 A), and Notch 3 was detected in both tumor and stromal cells (Fig. 1 A). Additionally, Hes1 and Hey2 were both detected in neoplastic cells (Fig. 1 B), and Hey2 also in intratumoral endothelial cells (Fig. 1 B). Many Notch pathway genes are direct transcriptional targets of NICD and thus can be used to determine pathway inhibition (Bray and Bernard, 2010). Accordingly,
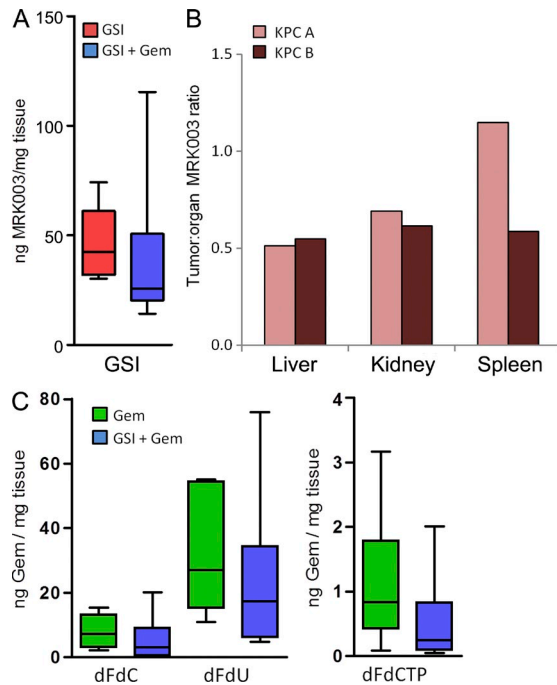
Figure 2. Intratumoral measurements of MRK003 and gemcitabine and tumor volumes. (A) Concentration of MRK003 in PDA tissue after monotherapy (*n* = 6) and GSI/gemcitabine combination treatment (*n* = 6; P = 0.18). (B) Ratio of MRK003 in other organs compared with the amount in a tumor in two different mice. (C) Concentration of gemcitabine and its metabolites in whole tumor samples (*n* = 6 on all cohorts). All animals were treated for 10 d then sacrificed 1 h after the last dose of gemcitabine and 6 h after the last dose of MRK003. Error bars represent SEM.

Hes1 mRNA was detected by in situ hybridization in neoplastic cells, and this decreased after treatment with MRK003 (Fig. 1 C). Bulk tumor tissue was also analyzed, and quantitative PCR of mRNA confirmed that MRK003 modulated a subset of Notch pathway genes, particularly those enriched in the stroma, including Jagged 1, Notch3, HeyL, and Hey1 (Fig. 1 D). Treatment with MRK003 was well tolerated by mice, despite the induction of goblet cell metaplasia (unpublished data) as previously reported for GSIs (van Es et al., 2005). Although Hes1 mRNA was not significantly decreased by MRK003 in total bulk tumor tissue, likely as a result of the contribution of stromal cells in KPC tumors as opposed to xenografts (Plentz et al., 2009), the intranuclear protein content of Hes1 was markedly diminished in normal intestinal and PDA cells (not depicted and Fig. 1 E). Therefore, both neoplastic cells and the tumor microenvironment in PanIN and PDA express components of the Notch pathway, and perturbations in the pathway can serve as pharmacodynamic biomarkers to antagonism by GSI.

Previous work from our laboratory has shown that PDA is hypovascular in both humans and the KPC model, and that improvement of gemcitabine delivery in the KPC model results in the prolongation of survival (Olive et al., 2009). Therefore, we determined whether the delivery of MRK003 or gemcitabine to PDA tumors was compromised. We found that the intratumoral level of MRK003 was within a therapeutically

relevant range (Fig. 2 A), albeit lower than MRK003 levels measured in the liver and kidney (Fig. 2 B). Interestingly, intratumoral MRK003 was modestly decreased by the co-administration of gemcitabine (Fig. 2 A). Using an LC/MS technique that we recently developed (Bapiro et al., 2011), we also determined that gemcitabine (dFdC [difluorode-oxycytidine]) and its inactive (dFdU [difluorodeoxyuridine]) and active (dFdCTP [difluorodeoxycytidine triphosphate]) metabolites were all slightly decreased in abundance after GSI treatment, albeit not significantly (Fig. 2 C). Therefore, MRK003 is delivered at therapeutic levels, but the concomitant administration of MRK003 and gemcitabine modestly antagonize the delivery of both agents.

MRK003/gemcitabine combination treatment significantly improves survival in the KPC model

Because we found that Notch signaling is prevalent in multiple cellular compartments in mouse pancreatic tumors, we examined a role for this pathway in tumor maintenance. A survival study was performed in KPC mice, as previously described (Olive et al., 2009), comparing vehicle, MRK003, and gemcitabine monotherapy cohorts to MRK003/gemcitabine combination–treated mice. Although there was no evidence of significant single agent activity of MRK003 or gemcitabine in PDA, the combination of MRK003 and gemcitabine synergistically and significantly improved anti-tumor efficacy and median survival in the KPC model (median survival vehicle 9 d vs. 26 d with GSI and gemcitabine; P = 0.002; Fig. 3 A). A prominent histological finding in the combination treatment group was the significant amount of necrosis in the combination-treated tumors (Fig. 3, B and C; P = 0.003). Unlike tumor core necrosis, which is commonly observed in xenograft tumors, in KPC tumors combination treatment induced necrosis that occurred in patches scattered throughout the tumor. Tumor volumes, measured with high resolution ultrasound, were calculated for all mice on study and tumor growth rate was estimated for each tumor and each cohort. There was no significant difference in tumor volumes at the start of treatment (unpublished data). Tumor shrinkage was not observed, although combination treatment with MRK003 and gemcitabine had a significant effect on halting tumor growth (P = 0.002; Fig. 3 D). We found no correlation between final tumor size and necrosis or treatment length and necrosis, particularly in the treatment cohorts that contained the GSI (unpublished data). Tissue obtained at endpoint of the survival studies revealed decreased proliferation and increased cell death in MRK003-treated mice but variable effects in the MRK003/gemcitabine cohort (unpublished data). To clarify the early effects of treatment, KPC tumors were examined after 10 d of treatment. MRK003 monotherapy significantly inhibited proliferation (P = 0.005; Fig. 3 E), and the combination of MRK003 and gemcitabine showed a trend toward decreased proliferation (P = 0.07; Fig. 3 E). Additionally, combination-treated KPC tumors had an elevated content of apoptotic cells in comparison to monotherapy (P = 0.02; Fig. 3 F) and control treatments (P = 0.008; Fig. 3 F). This increase in apoptosis was
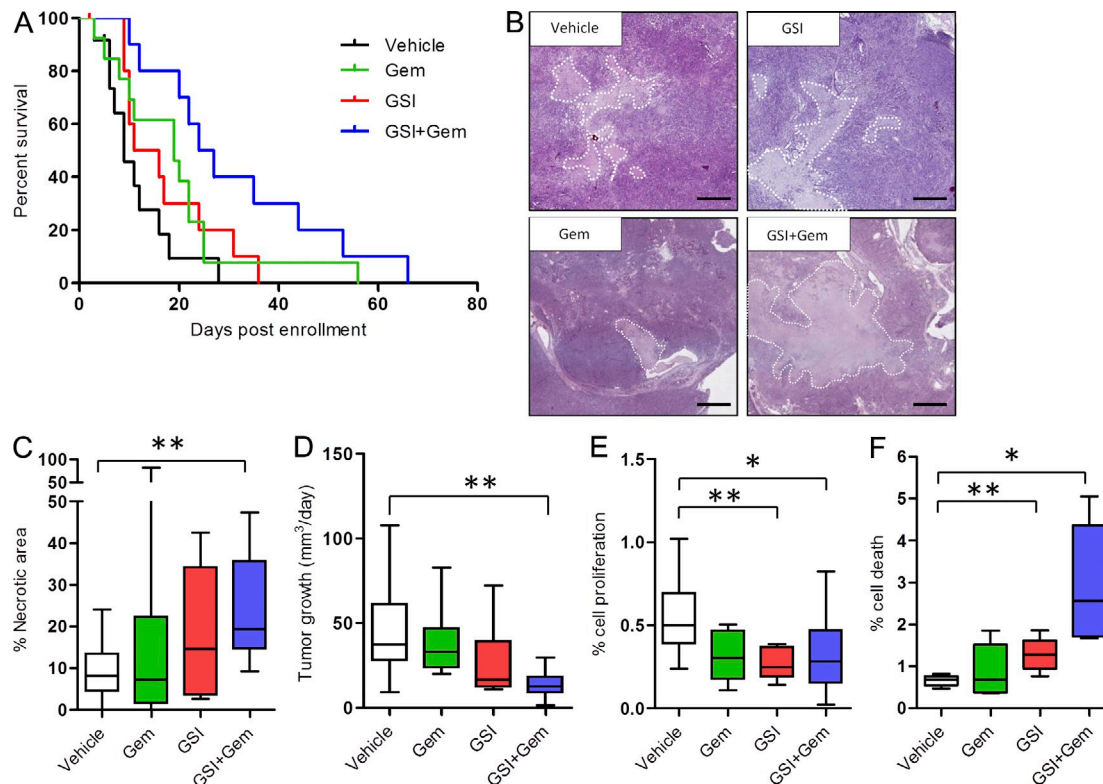
Figure 3. Combination treatment with MRK003 and Gemcitabine prolongs survival in PDA. (A) Survival is extended by the combination treatment of GSI and Gemcitabine (median survival vehicle 9 d vs. 26 d with GSI and gemcitabine; P = 0.002; n = 11 vehicle [black], n = 12 gemcitabine [green], n = 10 GSI [red], n = 10 GSI and gemcitabine [blue]). (B) Histological representative tumor appearances for each of the cohorts of animals treated in the survival study (bars, 200 μm). Necrotic areas are outlined. (C) Quantification of necrosis in the survival study (**, P = 0.003; n = 11 vehicle, n = 10 gemcitabine, n = 7 GSI, n = 9 GSI + gemcitabine). (D) Quantification of tumor volume growth using twice weekly high resolution ultrasound (**, P = 0.002; n = 10 in all cohorts). (E) Computer-based quantification of proliferation (phospho-histone histone H3) in tumors from mice treated for 10 d (**, P = 0.005; GSI n = 5, vehicle n = 10; *, P = 0.07; GSI + gemcitabine n = 6, vehicle n = 10). (F) Computer-based quantification of apoptosis in tumors from mice treated for 10 d (*, P = 0.008). Combination treatment (n = 6) group compared with vehicle (n = 5; **, P = 0.02), gemcitabine (n = 6), and GSI alone (n = 6; *, P = 0.01, GSI compared with vehicle). Error bars represent SEM.

also significantly different in the GSI–treated cohort compared with vehicle (P = 0.01; Fig. 3 F) and could not be attributed to stromal myofibroblasts (not depicted). Therefore, the combination of MRK003 and gemcitabine suppresses neoplastic cell proliferation and stimulates apoptosis and intratumoral necrosis.

MRK003/gemcitabine kills intratumoral endothelial cells and synergistically decreases vascular function and density in PDA

The vascular endothelium was also specifically assessed because the Notch pathway is implicated in vasculogenesis and tumor angiogenesis (Phng and Gerhardt, 2009). We found that treatment of KPC mice for 3 d with MRK003 alone and the combination of MRK003/gemcitabine rapidly induced endothelial cell death (P = 0.02 combination treatment compared with vehicle; Fig. 4, A and B). Indeed, the intratumoral vasculature was significantly less functional after MRK003/gemcitabine treatment as measured by perfusion of *Lycopersicon esculentum* lectin (P = 0.008 vs. vehicle; Fig. 4, C and D). To a lesser extent, MRK003 monotherapy treatment also revealed this property (Fig. 4, C and D). MRK003/gemcitabine combination treatment also significantly decreased the density

of intratumoral vessels within 3 d of treatment (Fig. 4, E and F). Notably, KPC intratumoral endothelial cells demonstrated decreased protein content of the Notch target genes Hey1 and Hey2 after MRK003 treatment (Fig. 4 G). Additionally, 2H11 mouse endothelial cells demonstrated decreased endothelial sprouting in culture after treatment with either gemcitabine or MRK003, with the combination providing the greatest effect. Examining the 2H11 cell lines also revealed a decrease in Jagged1 and Notch3 protein upon treatment with the GSI (unpublished data). Collectively, these findings show that MRK003 targets Notch signaling to decrease KPC endothelial cell survival and vascular function, and that this is exacerbated by combination treatment with gemcitabine.

Hypoxia sensitizes KPC tumor cells to growth inhibition by GSI

We reasoned that the reduced intratumoral vascular function and density after MRK003/gemcitabine treatment could compromise PDA tissue metabolism and survival. Accordingly, pimonidazole adduct formation was used to determine whether tissue oxygenation was limiting under these conditions (Raleigh et al., 1998). We found that MRK003/gemcitabine-treated KPC mice had a large increase (four- to fivefold) in tumor
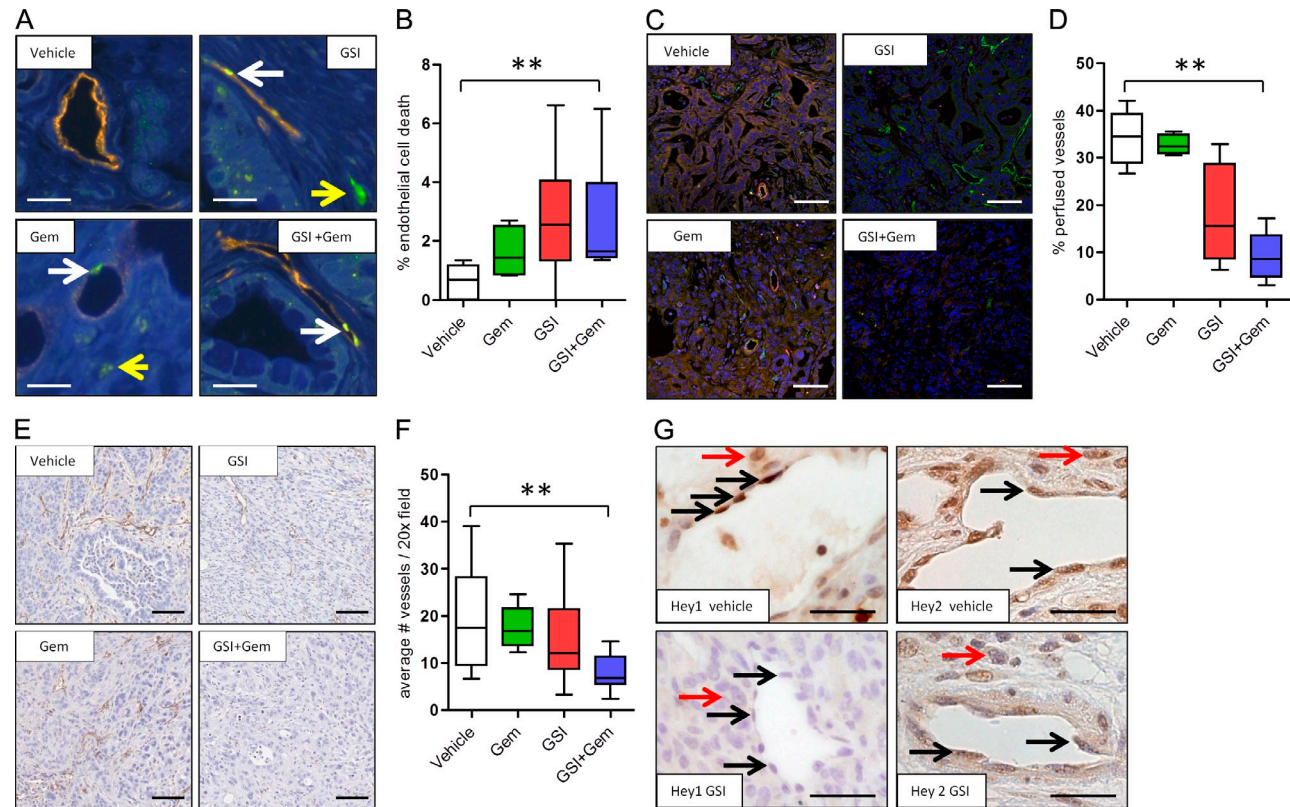
Figure 4. The combination of MRK003 and gemcitabine synergistically kills intratumoral endothelial cells to decrease vascular function and density in PDA. (A) Representative immunofluorescence images of DAPI (blue), Meca32 (orange), and Cleaved caspase 3 (CC3; green) content in each of the 3 d–treated cohorts ($n = 3$ or more samples evaluated for each cohort). White arrows: CC3-positive endothelial cells; yellow arrow: CC3-positive nonendothelial cell. Bars, 10 µm. (B) Percentage of CC3-positive Meca32-expressing endothelial cells in tumor samples treated for 3 d (**, P = 0.008). Vehicle, $n = 5$; gemcitabine, $n = 4$; GSI, $n = 6$; GSI and gemcitabine, $n = 6$. (C) Representative immunofluorescence images of DAPI (blue), Meca32 (green), and Lectin (red) content in each of the 3 d–treated cohorts (bars, 50 µm; $n = 3$ or more samples evaluated for each cohort). (D) Quantification of vascular patency (percentage of lectin and meca32 positive endothelial cells) in the GSI/gemcitabine combination treatment ($n = 5$) compared with vehicle ($n = 5$; **, P = 0.008) or gemcitabine ($n = 3$; P = 0.004) GSI ($n = 4$; P = 0.06) compared with vehicle. (E) Histological representative Meca32 IHC-stained images for each of the cohorts of animals treated for 10 d. Bars, 50 µm. (F) Quantification of MVD in 3 d cohorts reveals a significant decrease in MVD in the GSI/gemcitabine combination treatment ($n = 4$) cohort compared with the gemcitabine ($n = 4$; P = 0.03), GSI ($n = 4$; P = 0.03), and vehicle ($n = 8$; **, P = 0.02) cohorts. All animals were sacrificed 1 h after the last dose of gemcitabine and 6 h after the last dose of the GSI. (G) Expression of Hey1 and Hey2 protein in the tumor endothelial cells of mice treated with vehicle or GSI. Black arrows: positive endothelial nuclei; red arrows: positive nonendothelial KPC tumor nuclei. Bars, 10 µm. $n = 3$ for each cohort. Error bars represent SEM.

hypoxia (P = 0.006; Fig. 5, A and B). Interestingly, the amount of baseline hypoxia in vehicle-treated KPC tumors was almost undetectable (Fig. 5, A and B), despite the hypovascular state of this tissue (Olive et al., 2009). To determine whether the treatment efficacy of MRK003 and gemcitabine are influenced by relative oxygenation levels, tumor cells were placed under normoxic and hypoxic conditions and the cell viability was measured. Under normoxic conditions, cultured KPC tumor cell lines exhibited variable sensitivity to MRK003, with an IC50 ranging from 2 to >100 µM (Fig. 5, C and D). Interestingly, hypoxic culturing of the same PDA cells increased the cytotoxic effect of MRK003 by up to fivefold (Fig. 5 D), an effect which was also observed in HPAF (Fig. 5 E) and Panc-1 (not depicted) human pancreatic cancer cell lines. This finding was reminiscent of previous results indicating that colon cancer (Meng et al., 2009) and neuroblastoma cells (Stockhausen et al., 2005) in culture activate NICD-dependent transcription

in response to cytotoxic chemotherapy, thereby sensitizing cells to GSI treatment. In contrast, however, we found that PDA did not induce NICD-dependent transcription in response to gemcitabine treatment in vivo or in culture (unpublished data). Additionally, increased susceptibility to gemcitabine cytotoxicity was not observed in PDA cell lines upon hypoxic incubation (Fig. 5 F). Instead, in accordance with prior studies that used normal cells (Gustafsson et al., 2005) and neoplastic cells (Sahlgren et al., 2008; Chen et al., 2009), we found that hypoxia increased the mRNA expression of several NICD target genes, such as *Survivin* and *Notch 3* (Fig. 5 G). Survivin and Notch3 have established antiapoptotic roles (Mita et al., 2008; Indraccolo et al., 2009; Pradeep et al., 2011), and the hypoxia-induced elevations in *Survivin* and *Notch3* mRNA were selectively repressed by MRK003, providing a mechanistic basis for the sensitivity of PDA cells to GSI while under hypoxic conditions.
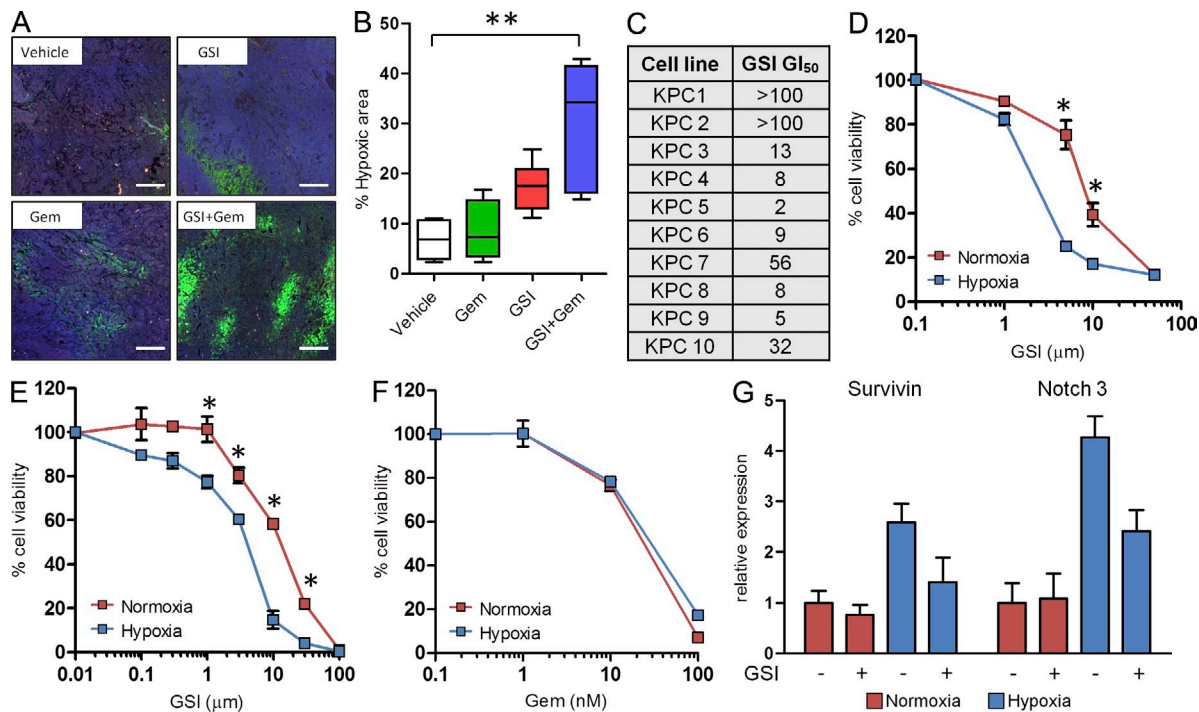
Figure 5. Treatment–induced hypoxia acutely sensitizes tumor cells to MRK003. (A) Representative immunofluorescence images of pimonidazole hydrochloride (Hypoxyprobe-1) staining with areas of hypoxia shown in bright green after 3 d of treatment (bars, 100 μm; $n = 4$ or more samples evaluated for each condition). (B) Levels of hypoxia in tumors treated with the combination treatment ($n = 6$) compared with vehicle ($n = 4$; **, $P = 0.006$) and gemcitabine ($n = 4$; $P = 0.02$) cohorts. Combination treatment was compared with GSI ($n = 6$; $P = 0.07$). GSI treatment was compared with vehicle ($P = 0.01$). (C) A panel of 10 KPC cell lines were tested to determine the GI50 values when treated with GSI under normoxia (units = μM). (D) KPC cell lines were examined for effects of GSI under normoxic and hypoxic conditions. The graph shown is representative of 10 cell lines. These experiments were performed in triplicate on three separate occasions (*, $P < 0.001$). (E) Human PDA cells were examined for effects of GSI under normoxic and hypoxic conditions. The graph shown is representative of the HPAF cell line. This experiment was performed in triplicate on two separate occasions (*, $P < 0.001$). (F) KPC cell lines were examined for the cytotoxic activity of gemcitabine under normoxic and hypoxic conditions. (G) qRT-PCR of survivin and Notch3 under hypoxia, and after incubation with MRK003. Error bars represent SEM.

Although we cannot exclude the roles for additional intracellular targets of GSIs (Kopan and Ilagan, 2004; Jorissen and De Strooper, 2010), or the effect upon stem-like cells in pancreatic tumors (Simeone, 2008; Pannuti et al., 2010), we demonstrate that the antivascular effects of GSIs are an important component in the response of KPC mice to MRK003, and that this is greatly exacerbated by the co-administration of gemcitabine, leading to vascular regression and intratumoral hypoxia. Additionally, although previous studies reported that Notch 1 and Notch2 regulated this pathway in similar mouse models of pancreatic cancer, we did not observe significant alterations in *Notch1* or *Notch2* mRNA levels in bulk tumor tissues in response to GSI (not depicted; Hanlon et al., 2010; Mazur et al., 2010). Rather, we observed decreases in Notch3 protein and mRNA after GSI treatment (Fig. 1, A and D).

We recently reported that stromal depletion with a smoothened inhibitor increased the vascular density in KPC tumors, leading to elevated gemcitabine delivery and response (Olive et al., 2009). Here, we show that MRK003 and gemcitabine effectively synergize to prolong survival in KPC mice, and that intratumoral gemcitabine delivery is actually hindered during treatment. Therefore, some therapeutics may enhance the cytotoxicity of gemcitabine to promote anti-tumor responses

in pancreatic cancer without increasing gemcitabine levels, and GSIs are an exemplar by targeting both endothelial and neoplastic cells in PDA and becoming more potent during the ensuing hypoxic necrosis.

This is the first study demonstrating that the dysfunctional vasculature in primary PDA tumors represents an attractive target for antivascular strategies. Indeed, prior preclinical work with genetically engineered mouse models (Singh et al., 2010), and multiple clinical trials that used anti-VEGF strategies, failed to show benefits in PDA (Van Cutsem et al., 2009; Kindler et al., 2010). This may reflect a greater dependency of PDA vasculature on the Notch pathway rather than VEGF-mediated signaling to maintain the intratumoral vasculature. The ability of GSIs to prevent pancreatic cancer in mouse models has previously been attributed to the antiproliferative affects of these agents (Plentz et al., 2009). Although we also find that MRK003 reduces the proliferation of neoplastic cells in established PDA tumors, this has a negligible impact upon disease progression. Rather, we find that MRK003 also destabilizes endothelial cells in established PDA tumors, and that in combination with gemcitabine promotes intratumoral vascular regression. We propose that the ensuing intratumoral hypoxia sensitizes the neoplastic cells to the effects of the GSI by targeting new biochemical dependencies,

such as *survivin* and *Notch3*, and provides an explanation for the tumor necrosis and synergistic disease prolongation observed in vivo. Therefore, our work supports the clinical investigation of GSIs in combination with gemcitabine for patients with PDA.

MATERIALS AND METHODS

Cell culture. Mouse pancreatic cancer cell lines were isolated from tumors arising in KPC mice using a modification of the protocol described by Schreiber et al. (2004). GI50 was assessed by plating 10^4 cells per well of a 96-well plate and culturing for 3 d in the presence or absence of drug. Cell viability was determined via CellTiter-Glo assay (Promega). For hypoxia experiments, cells were cultured in 1% oxygen in an Invivo2 500 Hypoxia Workstation (Ruskinn Life Sciences Ltd). Human pancreatic cell lines HPAF and Panc1 (American Type Culture Collection) were cultured in DME and 10% FBS.

Mouse strains. The KPC (K-ras^LSL-G12D, Trp53^LSL-R172H, PDX1-Cre) mouse has been described previously (Hingorani et al., 2005). All mice were housed according to institutional guidelines and UK Home Office requirements.

Antibodies. Commercial antibodies specific to Hes1 (MBL), Hey1 (Millipore), Hey2 (Millipore), Jag1 (Abcam), Dll4 (Abcam), Notch3 (Abcam), PH3 (Cell Signaling Technology), CC3 (Cell Signaling Technology), and MECA32 (Santa Cruz Biotechnology, Inc.) were used according to the manufacturers' recommendations.

Histology, immunohistochemistry, in situ hybridization, and immuno-fluorescence. Necropsies were performed on all animals and tissues stored as described previously (Olive et al., 2009). Formalin-fixed paraffin-embedded mouse pancreatic tissue was processed by standard methods or subjected to immunohistochemical staining as previously described (Olive et al., 2009). Hes1 IHC was performed with tyramide signal amplification (TSA kit; Invitrogen). Automated quantification was performed on 30 randomly chosen fields using the Ariol imaging system and analysis software (Genetix). Necrotic areas were manually outlined using Scanscope software (Imagescope), and then quantified using Aperio-scanned images of H&E sections cut through the center of each tumor. In situ hybridization was performed using standard internal protocols with a Hes1-specific antisense probe (Sasai et al., 1992).

Vascular labeling, drug diffusion, and hypoxyprobe. Vascular labeling and drug diffusion studies were performed as previously described (Olive et al., 2009). Hypoxyprobe-1 (HPI, Inc.) was given at 60 mg/kg via i.p. injection 1 h before sacrifice. Tissues were embedded in paraffin, sectioned, rehydrated, and stained with Hypoxyprobe-1MAb1 conjugated to FITC followed by goat anti-fluorescein Alexa Fluor 488 and counterstained with DAPI.

Quantitative PCR. Pancreatic tissue samples were immediately placed in an RNAlater solution (QIAGEN) and stored for at least 24 h at 4°C and then snap-frozen until processing. Total RNA was isolated using a Tissue-Lyser (QIAGEN) and RNeasy kit (QIAGEN). cDNA was synthesized from 1–2 μg RNA using the QPCR cDNA Synthesis kit (Applied Biosystems) and analyzed by quantitative real-time PCR on a 7900HT Real-Time PCR system using relative quantification (ΔΔct) with Taqman gene expression assays (Applied Biosystems). Actin was used as the endogenous control.

Immunoblotting. Tissue or cells were homogenized in SDS lysis buffer. DC/BCA Protein Assay (Bio-Rad Laboratories) was performed to determine protein concentration. Lysates were electrophoresed on 4–12% PAGE gels (Invitrogen), transferred to PVDF, and immunoblotted according to manufacturer's recommendations.

Drug formulation and delivery. Drug solutions were prepared fresh before each dose using a dounce homogenizer. MRK003, a GSI (Merck Research Laboratories), was synthesized according to standard medicinal chemistry procedures. For the in vitro experiments, stocks were prepared at 10 mM in DMSO and dilutions were made directly before use. For the in vivo

experiments, MRK003 was dosed as a suspension in 0.5% methylcellulose at a 10 ml/kg dosing volume, made fresh daily. Before administering each dose the compound was thoroughly mixed to distribute suspension evenly. The dosing schedule for MRK003 was 100 mg/kg by oral gavage, once daily for days 1–3 of each week, which was well tolerated. This schedule has been proven to be more tolerable to mouse models, and we therefore continued to use this schedule in our studies (Plentz et al., 2009). Gemcitabine was dosed as a solution in 0.9% normal saline at a 100 mg/kg solution, via intraperitoneal route, twice weekly as previously reported (Olive et al., 2009).

Pharmacokinetic analysis. Plasma, tumor, and normal tissue concentrations of MRK003 were evaluated by Merck Pharmaceuticals. Drug was isolated from homogenized tissue by acetonitrile extraction, and concentration determined by liquid chromatography–tandem mass spectrometry. All samples were processed by protein precipitation. 300 μl of the appropriate internal standard solution was added to each well containing sample, including the double blank sample where 300 μl acetonitrile was added. The samples were filtered, and then directly diluted with 600 μl of water and analyzed with an API 4000 mass spectrometer equipped with an electrospray interface. Gemcitabine, dFdU, and gemcitabine triphosphate were extracted from tumor tissue and quantified essentially as previously described (Bapiro et al., 2011).

Survival studies and Imaging. The structure for the survival study has been described previously (Olive et al., 2009) and was refined here by restricting enrolment to KPC mice that had tumors with a mean diameter between 6 and 9 mm. High resolution ultrasound imaging was performed as described previously (Olive et al., 2009).

Statistical analysis and quantification. Statistical analyses were performed using Prism version 5.00 for Windows (GraphPad Software). Histological analysis was either performed manually or using Ariol software (Leica) for quantification.

REFERENCES

Bapiro, T.E., F.M. Richards, M.A. Goldgraben, K.P. Olive, B. Madhu, K.K. Frese, N. Cook, M.A. Jacobetz, D.M. Smith, D.A. Tuveson, et al. 2011. A novel method for quantification of gemcitabine and its metabolites 2′,2′-difluorodeoxyuridine and gemcitabine triphosphate in tumour tissue by LC-MS/MS: comparison with (19)F NMR spectroscopy. *Cancer Chemother. Pharmacol.* 68:1243–1253. http://dx.doi.org/10.1007/s00280-011-1613-0

Beatty, G.L., E.G. Chiorean, M.P. Fishman, B. Saboury, U.R. Teitelbaum, W. Sun, R.D. Huhn, W. Song, D. Li, L.L. Sharp, et al. 2011. CD40 agonists alter tumor stroma and show efficacy against pancreatic carcinoma in mice and humans. *Science.* 331:1612–1616. http://dx.doi.org/10.1126/science.1198443

Bray, S., and F. Bernard. 2010. Notch targets and their regulation. *Curr. Top. Dev. Biol.* 92:253–275. http://dx.doi.org/10.1016/S0070-2153(10)92008-5

Burris, H.A. III, M.J. Moore, J. Andersen, M.R. Green, M.L. Rothenberg, M.R. Modiano, M.C. Cripps, R.K. Portenoy, A.M. Storniolo, P. Tarassoff, et al. 1997. Improvements in survival and clinical benefit with gemcitabine as first-line therapy for patients with advanced pancreas cancer: a randomized trial. *J. Clin. Oncol.* 15:2403–2413.

Chen, Y.Q., C.L. Zhao, and W. Li. 2009. Effect of hypoxia-inducible factor-1alpha on transcription of survivin in non-small cell lung cancer. *J. Exp. Clin. Cancer Res.* 28:29. http://dx.doi.org/10.1186/1756-9966-28-29

Fitzgerald, K., A. Harrington, and P. Leder. 2000. Ras pathway signals are required for notch-mediated oncogenesis. *Oncogene.* 19:4191–4198. http://dx.doi.org/10.1038/sj.onc.1203766

Gustafsson, M.V., X. Zheng, T. Pereira, K. Gradin, S. Jin, J. Lundkvist, J.L. Ruas, L. Poellinger, U. Lendahl, and M. Bondesson. 2005. Hypoxia requires notch signaling to maintain the undifferentiated cell state. *Dev. Cell.* 9:617–628. http://dx.doi.org/10.1016/j.devcel.2005.09.010

Hanlon, L., J.L. Avila, R.M. Demarest, S. Troutman, M. Allen, F. Ratti, A.K. Rustgi, B.Z. Stanger, F. Radtke, V. Adsay, et al. 2010. Notch1 functions as a tumor suppressor in a model of K-ras–induced pancreatic ductal adenocarcinoma. *Cancer Res.* 70:4280–4286. http://dx.doi.org/10.1158/0008-5472.CAN-09-4645

Hezel, A.F., A.C. Kimmelman, B.Z. Stanger, N. Bardeesy, and R.A. Depinho. 2006. Genetics and biology of pancreatic ductal adenocarcinoma. *Genes Dev.* 20:1218–1249. http://dx.doi.org/10.1101/gad.1415606

Hingorani, S.R., E.F. Petricoin, A. Maitra, V. Rajapakse, C. King, M.A. Jacobetz, S. Ross, T.P. Conrads, T.D. Veenstra, B.A. Hitt, et al. 2003. Preinvasive and invasive ductal pancreatic cancer and its early detection in the mouse. *Cancer Cell.* 4:437–450. http://dx.doi.org/10.1016/S1535-6108(03)00309-X

Hingorani, S.R., L. Wang, A.S. Multani, C. Combs, T.B. Deramaudt, R.H. Hruban, A.K. Rustgi, S. Chang, and D.A. Tuveson. 2005. Trp53R172H and KrasG12D cooperate to promote chromosomal instability and widely metastatic pancreatic ductal adenocarcinoma in mice. *Cancer Cell.* 7:469–483. http://dx.doi.org/10.1016/j.ccr.2005.04.023

Indraccolo, S., S. Minuzzo, M. Masiero, I. Pusceddu, L. Persano, L. Moserle, A. Reboldi, E. Favaro, M. Mecarozzi, G. Di Mario, et al. 2009. Cross-talk between tumor and endothelial cells involving the Notch3-Dll4 interaction marks escape from tumor dormancy. *Cancer Res.* 69:1314–1323. http://dx.doi.org/10.1158/0008-5472.CAN-08-2791

Jones, S., X. Zhang, D.W. Parsons, J.C. Lin, R.J. Leary, P. Angenendt, P. Mankoo, H. Carter, H. Kamiyama, A. Jimeno, et al. 2008. Core signaling pathways in human pancreatic cancers revealed by global genomic analyses. *Science.* 321:1801–1806. http://dx.doi.org/10.1126/science.1164368

Jorissen, E., and B. De Strooper. 2010. Gamma-secretase and the intramembrane proteolysis of Notch. *Curr. Top. Dev. Biol.* 92:201–230. http://dx.doi.org/10.1016/S0070-2153(10)92006-1

Kindler, H.L., D. Niedzwiecki, D. Hollis, S. Sutherland, D. Schrag, H. Hurwitz, F. Innocenti, M.F. Mulcahy, E. O'Reilly, T.F. Wozniak, et al. 2010. Gemcitabine plus bevacizumab compared with gemcitabine plus placebo in patients with advanced pancreatic cancer: phase III trial of the Cancer and Leukemia Group B (CALGB 80303). *J. Clin. Oncol.* 28:3617–3622. http://dx.doi.org/10.1200/JCO.2010.28.1386

Kopan, R., and M.X. Ilagan. 2004. Gamma-secretase: proteasome of the membrane? *Nat. Rev. Mol. Cell Biol.* 5:499–504. http://dx.doi.org/10.1038/nrm1406

Mazur, P.K., H. Einwächter, M. Lee, B. Sipos, H. Nakhai, R. Rad, U. Zimber-Strobl, L.J. Strobl, F. Radtke, G. Klöppel, et al. 2010. Notch2 is required for progression of pancreatic intraepithelial neoplasia and development of pancreatic ductal adenocarcinoma. *Proc. Natl. Acad. Sci. USA.* 107:13438–13443. http://dx.doi.org/10.1073/pnas.1002423107

Meng, R.D., C.C. Shelton, Y.M. Li, L.X. Qin, D. Notterman, P.B. Paty, and G.K. Schwartz. 2009. gamma-Secretase inhibitors abrogate oxaliplatin-induced activation of the Notch-1 signaling pathway in colon cancer cells resulting in enhanced chemosensitivity. *Cancer Res.* 69:573–582. http://dx.doi.org/10.1158/0008-5472.CAN-08-2088

Mita, A.C., M.M. Mita, S.T. Nawrocki, and F.J. Giles. 2008. Survivin: key regulator of mitosis and apoptosis and novel target for cancer therapeutics. *Clin. Cancer Res.* 14:5000–5005. http://dx.doi.org/10.1158/1078-0432.CCR-08-0746

Miyamoto, Y., A. Maitra, B. Ghosh, U. Zechner, P. Argani, C.A. Iacobuzio-Donahue, V. Sriuranpong, T. Iso, I.M. Meszoely, M.S. Wolfe, et al. 2003. Notch mediates TGF alpha-induced changes in epithelial differentiation during pancreatic tumorigenesis. *Cancer Cell.* 3:565–576. http://dx.doi.org/10.1016/S1535-6108(03)00140-5

Olive, K.P., M.A. Jacobetz, C.J. Davidson, A. Gopinathan, D. McIntyre, D. Honess, B. Madhu, M.A. Goldgraben, M.E. Caldwell, D. Allard, et al. 2009. Inhibition of Hedgehog signaling enhances delivery of chemotherapy in a mouse model of pancreatic cancer. *Science.* 324:1457–1461. http://dx.doi.org/10.1126/science.1171362

Pannuti, A., K. Foreman, P. Rizzo, C. Osipo, T. Golde, B. Osborne, and L. Miele. 2010. Targeting Notch to target cancer stem cells. *Clin. Cancer Res.* 16:3141–3152. http://dx.doi.org/10.1158/1078-0432.CCR-09-2823

Phng, L.K., and H. Gerhardt. 2009. Angiogenesis: a team effort coordinated by notch. *Dev. Cell.* 16:196–208. http://dx.doi.org/10.1016/j.devcel.2009.01.015

Plentz, R., J.S. Park, A.D. Rhim, D. Abravanel, A.F. Hezel, S.V. Sharma, S. Gurumurthy, V. Deshpande, C. Kenific, J. Settleman, et al. 2009. Inhibition of gamma-secretase activity inhibits tumor progression in a mouse model of pancreatic ductal adenocarcinoma. *Gastroenterology.* 136:1741–1749: e6. http://dx.doi.org/10.1053/j.gastro.2009.01.008

Pradeep, C.R., W.J. Köstler, M. Lauriola, R.Z. Granit, F. Zhang, J. Jacob-Hirsch, G. Rechavi, H.B. Nair, B.T. Hennessy, A.M. Gonzalez-Angulo, et al. 2011. Modeling ductal carcinoma in situ: a HER2-Notch3 collaboration enables luminal filling. *Oncogene.* In press.

Raleigh, J.A., S.C. Chou, L. Tables, S. Suchindran, M.A. Varia, and M.R. Horsman. 1998. Relationship of hypoxia to metallothionein expression in murine tumors. *Int. J. Radiat. Oncol. Biol. Phys.* 42:727–730. http://dx.doi.org/10.1016/S0360-3016(98)00329-0

Sahlgren, C., M.V. Gustafsson, S. Jin, L. Poellinger, and U. Lendahl. 2008. Notch signaling mediates hypoxia-induced tumor cell migration and invasion. *Proc. Natl. Acad. Sci. USA.* 105:6392–6397. http://dx.doi.org/10.1073/pnas.0802047105

Sasai, Y., R. Kageyama, Y. Tagawa, R. Shigemoto, and S. Nakanishi. 1992. Two mammalian helix-loop-helix factors structurally related to Drosophila hairy and Enhancer of split. *Genes Dev.* 6:2620–2634. http://dx.doi.org/10.1101/gad.6.12b.2620

Schreiber, F.S., T.B. Deramaudt, T.B. Brunner, M.I. Boretti, K.J. Gooch, D.A. Stoffers, E.J. Bernhard, and A.K. Rustgi. 2004. Successful growth and characterization of mouse pancreatic ductal cells: functional properties of the Ki-RAS(G12V) oncogene. *Gastroenterology.* 127:250–260. http://dx.doi.org/10.1053/j.gastro.2004.03.058

Simeone, D.M. 2008. Pancreatic cancer stem cells: implications for the treatment of pancreatic cancer. *Clin. Cancer Res.* 14:5646–5648. http://dx.doi.org/10.1158/1078-0432.CCR-08-0584

Singh, M., A. Lima, R. Molina, P. Hamilton, A.C. Clermont, V. Devasthali, J.D. Thompson, J.H. Cheng, H. Bou Reslan, C.C. Ho, et al. 2010. Assessing therapeutic responses in Kras mutant cancers using genetically engineered mouse models. *Nat. Biotechnol.* 28:585–593. http://dx.doi.org/10.1038/nbt.1640

Smit, V.T., A.J. Boot, A.M. Smits, G.J. Fleuren, C.J. Cornelisse, and J.L. Bos. 1988. KRAS codon 12 mutations occur very frequently in pancreatic adenocarcinomas. *Nucleic Acids Res.* 16:7773–7782. http://dx.doi.org/10.1093/nar/16.16.7773

Stanger, B.Z., B. Stiles, G.Y. Lauwers, N. Bardeesy, M. Mendoza, Y. Wang, A. Greenwood, K.H. Cheng, M. McLaughlin, D. Brown, et al. 2005. Pten constrains centroacinar cell expansion and malignant transformation in the pancreas. *Cancer Cell.* 8:185–195. http://dx.doi.org/10.1016/j.ccr.2005.07.015

Stockhausen, M.T., J. Sjölund, C. Manetopoulos, and H. Axelson. 2005. Effects of the histone deacetylase inhibitor valproic acid on Notch signalling in human neuroblastoma cells. *Br. J. Cancer.* 92:751–759. http://dx.doi.org/10.1038/sj.bjc.6602309

Van Cutsem, E., W.L. Vervenne, J. Bennouna, Y. Humblet, S. Gill, J.L. Van Laethem, C. Verslype, W. Scheithauer, A. Shang, J. Cosaert, and M.J. Moore. 2009. Phase III trial of bevacizumab in combination with gemcitabine and erlotinib in patients with metastatic pancreatic cancer. *J. Clin. Oncol.* 27:2231–2237. http://dx.doi.org/10.1200/JCO.2008.20.0238

van Es, J.H., M.E. van Gijn, O. Riccio, M. van den Born, M. Vooijs, H. Begthel, M. Cozijnsen, S. Robine, D.J. Winton, F. Radtke, and H. Clevers. 2005. Notch/gamma-secretase inhibition turns proliferative cells in intestinal crypts and adenomas into goblet cells. *Nature.* 435:959–963. http://dx.doi.org/10.1038/nature03659